Negative electron-electron drag between narrow quantum Hall channels

H. C. W. Tso and D. J. W. Geldart
Department of Physics, Dalhousie University, Halifax, Nova Scotia, Canada B3H 3J5

P. Vasilopoulos
Department of Physics, Concordia University, 1455 de Maisonneuve Boulevard West, Montréal, Québec, Canada H3G 1M8

(Received 9 October 1997)

Momentum transfer due to Coulomb interaction between two parallel, two-dimensional, *narrow*, and spatially separated layers, when a current $I_{\rm drive}$ is driven through one layer, is studied in the presence of a perpendicular magnetic field B. The current induced in the drag layer $I_{\rm drag}$ is evaluated self-consistently with $I_{\rm drive}$ as a parameter. $I_{\rm drag}$ can be positive or negative depending on the value of the filling factor ν of the highest occupied bulk Landau level (LL). For a fully occupied LL, $I_{\rm drag}$ is *negative*, (i.e., it flows opposite to $I_{\rm drive}$), whereas it is positive for a half-filled LL. When the circuit is opened in the drag layer, a voltage $\Delta V_{\rm drag}$ develops in it; it is negative for a half-filled LL and positive for a fully occupied LL. This *positive* $\Delta V_{\rm drag}$, expressing a *negative* Coulomb drag, results from energetically favored *near-edge inter-LL transitions* that occur when the highest occupied bulk LL and the LL just above it become degenerate.
[S0163-1829(98)07707-8]

I. INTRODUCTION

Recently the transresistance R_T between two parallel two-dimensional (2D) systems[1–4] has been studied extensively due to advances in measuring[5] techniques. In most previous studies[1–5] only wide systems were considered, in which edge effects can be ignored. However, edge effects become prominent in narrow systems especially when a magnetic field B is present and the highest bulk LL is completely occupied. The electronic edge states are very different from the bulk states. For instance, if a weak random impurity potential is present, the bulk states are disordered[7] and occur in a series of energy bands of finite width $\Gamma_n(k)$, centered about the LL's with no states in the region between them. On the other hand, the edge states are degenerate with respect to the LL's. This can lead to profound differences in transport properties between the case when the highest bulk LL is completely occupied and that when it is not.

In this paper we study the influence of edge states on the drag by solving *self-consistently* the Coulomb-coupled Schrödinger equations for two *narrow* Hall bars. This goes substantially beyond the simple, not self-consistent treatments of Ref. 6 that used a parabolic confining potential. Here the potential is evaluated self-consistently from an initial square-well potential. We find that a current I_i is always induced in the direction of $I_{\rm drive}$ and the Coulomb interaction lifts the degeneracy of all occupied edge LL's, but not that of unoccupied and neighboring-occupied edge LL's. The Coulomb drag obtained is *two-to-three orders of magnitude larger* than that in zero field due to the increase in the available density of states when an external magnetic field is present. As the filling factor ν of the highest LL approaches 1, *near-edge inter-LL transitions* occur between this LL and that just above it. These transitions make $I_{\rm drag}$ or $\Delta V_{\rm drag}$ change sign when the circuit in the drag layer is closed or open, respectively. Thus, this negative drag is neither due to a thermal gradient[8] nor to an electron-hole coupling.

In the next section we present the formalism. In Sec. III we present and discuss the numerical results. We conclude with remarks in Sec. IV.

II. FORMALISM

A. Coupled Schrödinger equations

Consider two quantum Hall bars parallel to the (x,y) plane, separated by a distance d along the z axis, of thickness zero, width $L_x=w$, and length $L_y\equiv L\gg\ell_c$. The electrons are confined along x by infinitely high potential barriers. In a field $\mathbf{B}=-B\hat{\mathbf{z}}$, the electron wave function in the drive layer a, when the circuit in the y direction is closed, has the form $\psi^a_{nk}(x)e^{iky}/\sqrt{L}$ and ψ^a obeys

$$-\left(\frac{\hbar^2}{2m^*}\frac{\partial^2}{\partial x^2}+\frac{\hbar^2}{2m^*}(k-x/\ell_c^2)^2-e^{*2}\phi_{ab}(x)\right)\psi^a_{nk}(x)=E^a_{nk}\psi^a_{nk}(x). \tag{1}$$

The corresponding wave function $\psi^b_{nk}(x)$ in the drag layer b obeys

$$-\left(\frac{\hbar^2}{2m^*}\frac{\partial^2}{\partial x^2}+\frac{\hbar^2}{2m^*}(k-x/\ell_c^2)^2-e^{*2}\phi_{ba}(x)\right)\psi^b_{nk}(x)=E^b_{nk}\psi^b_{nk}(x). \tag{2}$$

Here n is the LL number, m^* is the effective mass, $\ell_c=\sqrt{\hbar/eB}$ is the magnetic length, e^* is equal to $e/\sqrt{\epsilon}$, and ϵ is the dielectric constant. For simplicity spin is neglected. The Coulomb potential ϕ_{ab} is given by

$$\phi_{ab}(x)=-2\int dx'[\,\delta\rho_a(x')\ln|x-x'|+\delta\rho_b(x')\ln\sqrt{(x-x')^2+d^2}\,]. \tag{3}$$

As for the charge densities ρ_a and ρ_b, they are given by

$$\rho_a(x)=\frac{1}{2\pi}\sum_n \int_{-k_0}^{k_0} dk\; g_n^a(k)|\psi_{nk}^a(x)|^2 f(E_{nk+\delta k}^a), \quad (4)$$

in the drive layer[9] and by

$$\rho_b(x)=\frac{1}{2\pi}\sum_n \int_{-k_0}^{k_0} dk\; g_n^b(k)|\psi_{nk}^b(x)|^2 f(E_{nk}^b), \quad (5)$$

in the drag layer. In Eqs. (3)–(5), $\delta\rho_\alpha(x)=\rho_\alpha(x)-\rho_{0\alpha}$, $\alpha=a$ or b, $\rho_{0\alpha}$ is the background charge density, f is the Fermi function, and $k_0=w/2\ell_c^2$. Notice that $\delta k=0$ in Eq. (5) since no current flows through in the drag layer. We take the effective background densities as equal, $\rho_{0a}=\rho_{0b}$, and constant. The Schrödinger equations for the drive and drag layers are solved self-consistently.

The weight function $g_n^a(k)$ depends on E_{nk}^a and expresses the degeneracy of the LL's. When the nth LL is completely filled, we have $g_n^a(k)=1$. When it is partially filled, we determine $g_n^a(k)$ self-consistently[10] from E_{nk}^a and the level broadening $\Gamma_n^a(k)$ due to scatterers from the assumptions (i) $\Gamma_n^a(k)$ is independent of k, and (ii) the total neutrality of the Hall bar and the local neutrality at its center are maintained. The meaning of these assumptions becomes clear if we consider two limiting cases for the average filling factor of the highest LL $\bar{\nu}\neq 1$. First, for an infinitely wide bar without edges, the energy levels E_{nk}^α is definitely degenerate with respect to the wave vector k and everywhere we have the same filling factor $\nu=\bar{\nu}$. Secondly, for a *narrow* Hall bar without the k degeneracy in E_{nk}^α and $g_n^\alpha(k)=1$, all k states are occupied if $\bar{\nu}=1$. But if $\bar{\nu}<1$, not all k states are occupied and electrons prefer those low-lying energy states near the center of the bar. Therefore the actual width of the Hall bar, defined by the density of electrons, will shrink to roughly $\bar{\nu}W$ and in it the filling factor is still 1 even though $\bar{\nu}$ is less than 1. In reality, there is scattering that broadens E_{nk}^α by, say, $\Gamma_n^\alpha(k)$. Within $\Gamma_n^\alpha(k)$, we assume that each k has the same electron occupancy, so the local filling factor depends on the local density of states at k. This average electron occupancy depends on the density of states $N_n(k)$ and is reflected in

$$g_n(k)=\frac{\bar{\nu}_n N_n(0)}{N_n(k)}[1-\Theta(\bar{\nu}_n N_n(0)-N_n(k))] + \Theta(\bar{\nu}_n N_n(0)-N_n(k)), \quad (6)$$

where $\Theta(x)$ is the Heaviside step function and $\bar{\nu}_n$ is the filling factor of the nth LL. Consequently, the electron density is nonzero within the width of the bar with local filling factor $\nu\neq 1$. At the center of the bar, which corresponds roughly to $k=0$, we have $g_n(k)=\bar{\nu}_n$. This ensures the neutrality at the center, which is in contrast with the single-layer treatment of Ref. 9, where only the total neutrality was preserved and only the $\nu=1$ situation could be handled. In our case, this local neutrality at the center ensures that $E_{nk}=(n+1/2)\hbar\omega_c$ at $k=0$. In Eq. (4), $\delta k\|y$ is the shift of the Fermi surface[9] that results from the application of a current $I_{\text{drive}}\|y$ through the drive layer in the presence of scattering.

B. Currents

The drive and induced currents, I_{drive} and I_i, are given by

$$I_{\text{drive}}=-I_0 w^2\sum_n \int dx \int_{-k_0}^{k_0} dk\; g_n^a(k) \times(k-x/\ell_c^2)|\psi_{n,k}^a(x)|^2 f(E_{n,k+\delta k}^a), \quad (7)$$

and

$$I_{\text{i}}=-I_0 w^2\sum_n \int dx \int_{-k_0}^{k_0} dk\; g_n^b(k) \times(k-x/\ell_c^2)|\psi_{nk}^b(x)|^2 f(E_{nk}^b), \quad (8)$$

where $I_0=e\hbar/2\pi m^* w^2$. I_{i} consists not only of the current induced by momentum transfer but also of the classical $\mathbf{E}\times\mathbf{B}$ drift[11] current in the direction of $\mathbf{B}\times\langle\mathbf{E}\rangle$ where $\langle\mathbf{E}\rangle$ is the average of a finite electrostatic field $\mathbf{E}$ exerted on the drag electrons by the charges that accumulate at the edges of the drive layer and produce the Hall voltage. This field $\mathbf{E}$ opens up the circular orbit of the drag electrons by accelerating those moving opposite to it and decelerating those moving in its direction.[11] Thus it induces an average current I_{es} in the direction of I_{drive} parallel to $\mathbf{B}\times\langle\mathbf{E}\rangle$ given by

$$I_{\text{es}}=-I_0 w^2\sum_n \int dx \int_{-k_0}^{k_0} dk\; g_n^0(k) \times(k-x/\ell_c^2)|\chi_{nk}(x)|^2 f(E_{nk}^0), \quad (9)$$

and $\chi_{nk}(x)$ obeys Eq. (1) with $a\to b$, $\phi\to\bar{\phi}$, $\rho\to\bar{\rho}$, and $E\to\bar{E}$. $\bar{\phi}(x)$ is given by Eq. (2) with the changes $\rho_a\to\bar{\rho}_b$, $\rho_b\to\rho_a$, and

$$\bar{\rho}_b(x)=\frac{1}{2\pi}\sum_n \int_{-k_0}^{k_0} dk\; g_n^0(k)|\chi_{nk}(x)|^2 f(E_{nk}^0). \quad (10)$$

The use of the equilibrium energy E_{nk}^0 in the drag layer to derive $g_n^0(k)$ and of the Fermi function in Eq. (9) eliminates electron transitions between different k's. Thus the current due to momentum transfer is

$$I_{\text{drag}}=I_i-I_{\text{es}}. \quad (11)$$

For fully occupied LL's we have $g_n^0(k)=g_n^b(k)=1$ and I_{drag} vanishes but the classical $\langle\mathbf{E}\rangle\times\mathbf{B}$ drift I_{es} does not.

C. Explicit relation between the drag current and drag voltage

When the circuit in the drag layer is opened, apart from the voltage induced by the $\langle\mathbf{E}\rangle\times\mathbf{B}$ drift, a drag voltage $\Delta V_{\text{drag}}=LI_{\text{drag}}\Delta t\,\delta(z)/\epsilon W$ develops along the bar as shown in Fig. 1. In a short time Δt it produces an intermediate current,

$$I_{\text{int}}=\frac{\rho_0 e\Delta V_{\text{drag}}}{B}=\Delta V_{\text{drag}}\frac{(n_{\max}+\nu)e^2}{2\pi\hbar}, \quad (12)$$

across the width, due to the $\mathbf{E}_{\text{drag}}\times\mathbf{B}$ drift. This results in an electric field $E_{\text{int}}=I_{\text{int}}\delta(z)\,\delta t/\epsilon L$, across the width, which produces another $\mathbf{E}_{\text{int}}\times\mathbf{B}$-drift current *opposite* to I_{drag}. The steady state is reached when these two currents are equal so that all the $\mathbf{E}\times\mathbf{B}$ drifts are balanced. Thus, E_{int} is given by

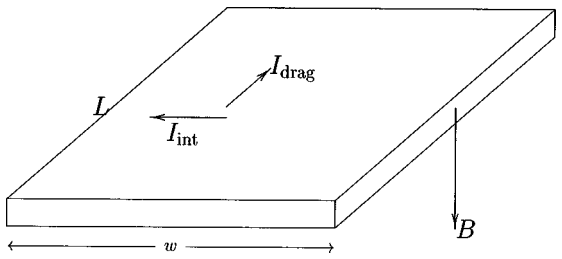

FIG. 1. Schematics of a quantum Hall bar, of length L and of width W, in a perpendicular magnetic field B. The currents $I_{\rm drag}$ and $I_{\rm int}$ are explained in the text.

$$E_{\rm int}=\frac{e^2(n_{\rm max}+\nu)}{2\pi\hbar\,\epsilon L}\Delta V_{\rm drag}\Delta t\,\delta(z)=\frac{2\pi\hbar}{e^2 w(n_{\rm max}+\nu)}I_{\rm drag} \tag{13}$$

with $n_{\rm max}$ the highest occcupied bulk LL number. The drag voltage is then

$$\Delta V_{\rm drag}=-\frac{2\pi\hbar}{(n_{\rm max}+\nu)e^2}\frac{L}{w}I_{\rm drag}, \tag{14}$$

where the minus sign is inserted according to the usual Ohm's law convention; $I_{\rm drag}$ is given by Eq. (9).

III. RESULTS AND DISCUSSION

We consider a GaAs sample at zero temperature, with $d=5\ell_c$, $w=20\ell_c$, and B chosen such that $\ell_c=100$ Å. The Schrödinger equations for the drive and drag layers are solved self-consistently and the average electron and current densities of the drag layer, with $n_{\rm max}=1$ and $\nu=0.5$, are plotted in Fig. 2. The solid and dotted curves represent equilibrium and nonequilibrium quantities, respectively. Figure 3 shows that the current density of the main figure is not symmetric. E^0_{nk} and $g^0_n(k)$ are shown in Fig. 4. The rapid change of $g^0_n(k)$ near the edges reflects the structure of the boundaries between edge and disordered bulk states. As shown in

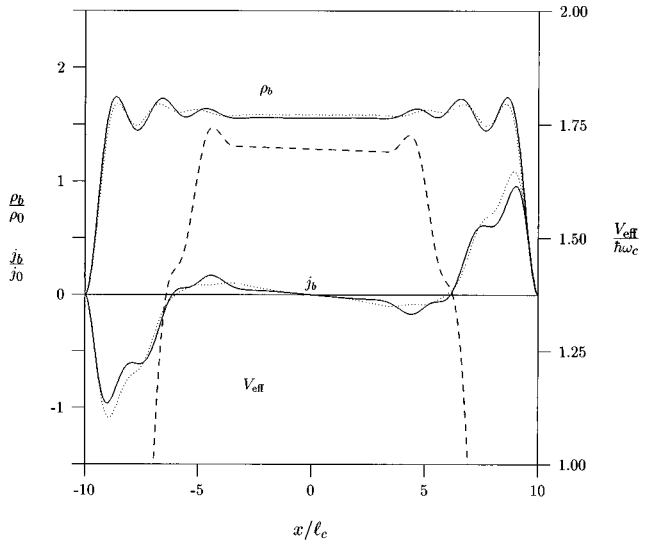

FIG. 2. Equilibrium (solid curves) and nonequilibrium (dotted curves) densities and current densities as a function of x for $n_{\rm max}=1$, $\nu=0.5$ with $j_0\equiv e\omega_c/2\pi\ell_c$ and $\rho_0\equiv 1/2\pi\ell_c^2$. The dashed curve is the effective potential $V_{\rm eff}$.

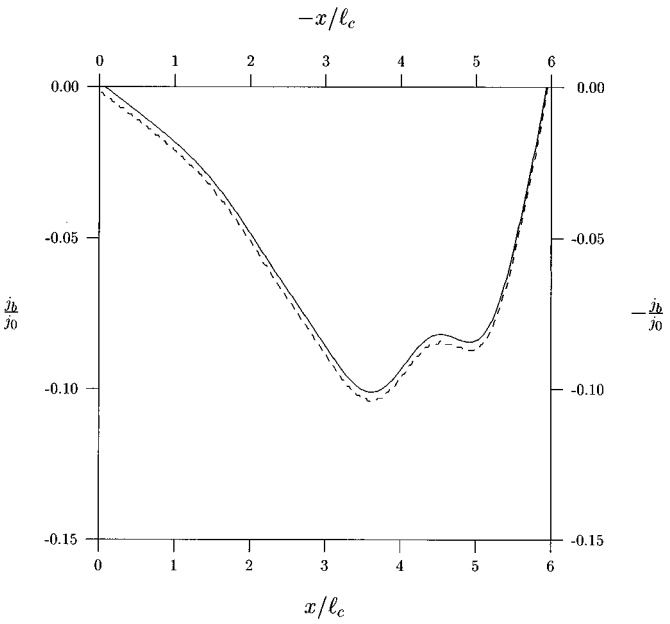

FIG. 3. Nonequilibrium current density as a function of x for $n_{\rm max}=1$, $\nu=0.5$. The solid curve refers to the bottom-left scales and the dashed curve to the top-right scales.

Fig. 2, the current-density (j_b) plot has qualitatively five different zones, namely, the outer-edge ($10\ell_c>|x|>6\ell_c$) and inner-edge ($6\ell_c>|x|>3.5\ell_c$) zones on both sides of the bar, and one bulk zone ($3.5\ell_c>|x|>0$). In the outer-edge zone j_b is opposite to that in the inner-edge zone and in the bulk zone it is negligible.

To understand the results of Fig. 2 we consider the single-electron motion. We first treat the equilibrium case ($I_{\rm drive}=0$, $\delta k=0$). For finite **B**, j_b near the edge is affected by the sharp changes of the electron density $n(x)$ and of the effective confining potential. Near the left edge, the gradient $\nabla n(x)$ is so large that there are more electrons, with guiding center at $x+\delta x$, e.g., near the maximum of $n(x)$ at $x<-9\ell_c$, flowing into the paper (y direction) than adjacent

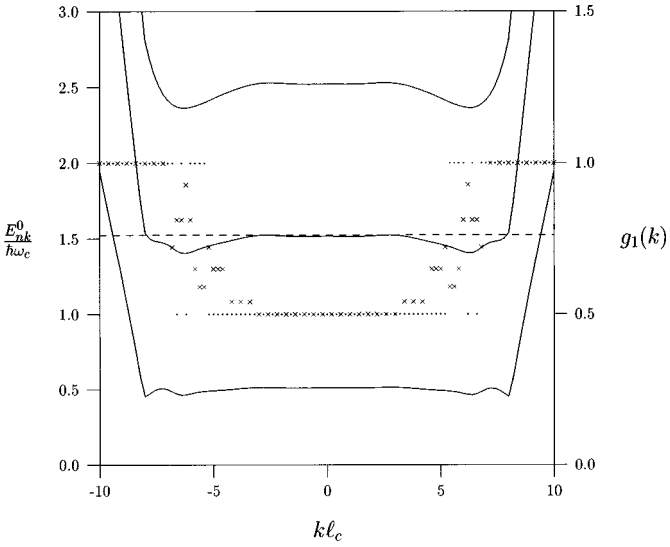

FIG. 4. Equilibrium LL energies and the weight function as a function of k for $n_{\rm max}=1$, $\nu=0.5$. The dashed line is the chemical potential. The dots correspond to $g^0_1(k)$ and the crosses to $g^b_1(k)$.

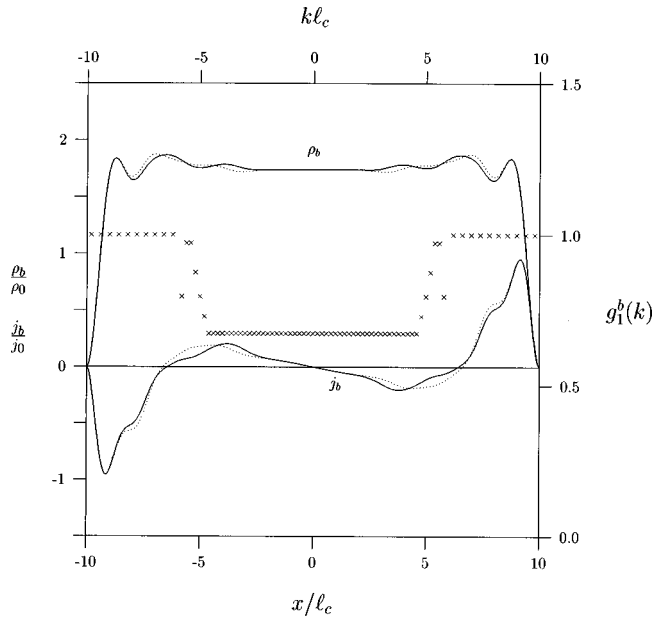

FIG. 5. Equilibrium (solid curves) and nonequilibrium (dotted curves) densities and current densities, as a function of x, and nonequilibrium weight function (crosses) as a function of k for $n_{\max}=1$, $\nu=0.8$.

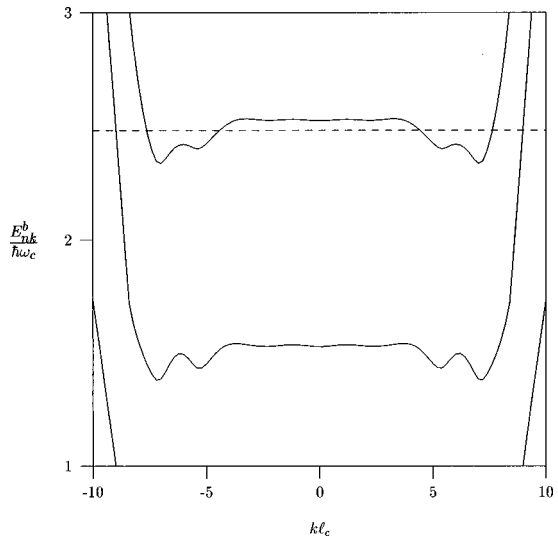

FIG. 6. Nonequilibrium LL energies as a function of k for $n_{\max}=1$, $\nu=1$. The dashed line is the chemical potential.

electrons, with guiding center at $x-\delta x$, flowing out of the paper; this gives rise to a local j_b, at x, in the negative y direction. This diamagnetic-drift current is thus proportional[11] to $\nabla n(x)$. In the same region the local effective electric field $\mathbf{E}_{\rm eff}=-\nabla V_{\rm eff}$, produced by electrons in the center of the bar, pushes the electrons towards the edge. This produces a $\mathbf{E}_{\rm eff}\times\mathbf{B}$-drift current[11] pointing in the same direction as the diamagnetic-drift current. However, for electrons located further away from the edges $\mathbf{E}_{\rm eff}$ changes direction. It pushes the electrons away from the edge towards the center of the bar, and produces a $\mathbf{E}_{\rm eff}\times\mathbf{B}$ drift j_b, proportional[11] to $\nabla V_{\rm eff}(x)=-\mathbf{E}_{\rm eff}$ that points in the *positive* (negative) y direction at the left (right) edge. In most of the outer-edge region, the $\mathbf{E}_{\rm eff}\times\mathbf{B}$ drift is comparable to the diamagnetic-drift whereas in the inner-edge region the $\mathbf{E}_{\rm eff}\times\mathbf{B}$ drift dominates. As for the bulk zone, $\nabla n(x)$ and $\nabla V_{\rm eff}(x)$ are almost zero and so is j_b. If we define the average drift velocities carried by the outer-left-edge, inner-left-edge, inner-right-edge, and outer-right-edge currents as $-v_{\rm out}^l$, $v_{\rm in}^l$, $-v_{\rm in}^r$, and $v_{\rm out}^r$, respectively, with corresponding average electron densities $n_{\rm out}^l$, $n_{\rm in}^l$, $n_{\rm in}^r$, and $n_{\rm out}^r$, the total current density is

$$I_i\sim n_{\rm out}^r v_{\rm out}^r-n_{\rm out}^l v_{\rm out}^l+n_{\rm in}^l v_{\rm in}^l-n_{\rm in}^r v_{\rm in}^r. \tag{15}$$

When no current is driven ($I_{\rm drive}=0$), we have $n_{\rm out}^r=n_{\rm out}^l$, $n_{\rm in}^r=n_{\rm in}^l$, $v_{\rm out}^r=v_{\rm out}^l$, $v_{\rm in}^r=v_{\rm in}^l$, or, in other words, the current density on the left edge balances out that on the right edge and thus $I_i=0$. When $I_{\rm drive}$ is switched on ($\delta k\neq 0$), E_{nk}^b and $g_n^b(k)$ change. This affects the drag electrons in two ways. First, on the average there are more electrons at $x>0$ than at $x<0$ due to $\phi^b(x)$, i.e., $n_{\rm in}^r+n_{\rm out}^r>n_{\rm in}^l+n_{\rm out}^l$ and this leads to an imbalance of j_b. Second, the inner-edge zone, shown in Fig. 2, expands into the bulk zone due to the change in $g_n^b(k)$. The resulting total $I_{\rm drag}$ is parallel to $I_{\rm drive}$ for $\nu=0.5$. As ν increases, the inner-edge zone expands further, due to the increase of $g_n^b(k)$ in the bulk zone (the guiding-center coordinate is proportional to k), as contrasting Fig. 2 with Fig. 5 shows; there is an increase in both $n_{\rm in}^l$ and $n_{\rm in}^r$ with $n_{\rm in}^l<n_{\rm in}^r$ and thus $I_{\rm drag}$ decreases for ν integer.

As ν approaches an integer, $g_n^b(k)\to 1$ in the bulk is the same as that in the edge zones and there is no bulk activity contributing to the drag current. However, the eigenvalues E_{nk}^b, shown in Fig. 6, with $n=n_{\max}$ near $kl_c=9$ and $n=n_{\max}+1$ near $kl_c=7$, are degenerate. Now the electrons prefer to occupy the inner-edge zone, lower-energy sites, with $n_{\max}+1$ and $4.8<|k_2\ell_c|<7.6$, rather than the outer-edge zone, higher-energy sites, with $n_{\max}$ and $|k_1\ell_c|>8.8$. This results in the current density shown in Fig. 7. Since the drag current is the total induced current minus the classical $\langle\mathbf{E}\rangle\times\mathbf{B}$ drift, we view these empty states as holes in the $n_{\max}$th LL responsible for $I_{\rm drag}$. These holes are responsible

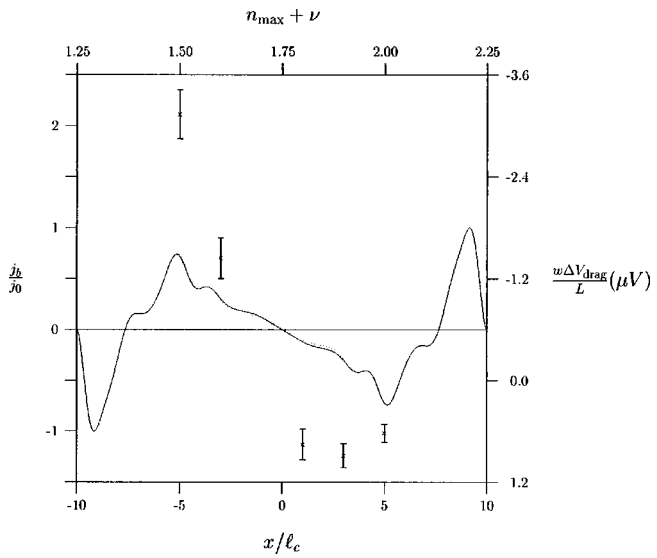

FIG. 7. Bottom-left scales: Equilibrium (solid curves) and nonequilibrium (dotted curves) current densities as a function of x for $n_{\max}=1$, $\nu=1$. Top-right scales: The drag voltage $\Delta V_{\rm drag}$ (crosses) as a function of ν with $n_{\max}=1$ and $I_{\rm drive}\simeq 0.08$ μA.

for the outer-edge currents. Since there are more holes at the left edge than at the right edge and holes are moving opposite to the outer-edge electrons of the drive layer, the induced current flows opposite to that due to electrons. On the other hand, electrons in the inner-edge zones of the $n_{\max}+1$ LL have a total current in the same direction as that due to the holes. When the sum of these two currents exceeds that due to electrons in the bulk $n_{\max}$th LL, the total current $I_{\rm drag}$, calculated by integrating $j_b(x)$ over the Hall bar, flows opposite to $I_{\rm drive}$ in contrast with the $B=0$ case, where it flows in the direction of $I_{\rm drive}$ for two electron layers. Accordingly, the drag voltage, shown on the right axis of Fig. 5, changes sign when ν approaches 1 and has a minimum in the vicinity of $\nu=1$. This change of sign occurs also in $I_{\rm drag}$, when allowed to flow, as Eq. (12) shows.

The predicted *negative* Coulomb drag can best be tested in an open-circuit configuration, i.e., by measuring the voltage difference along the bar to avoid the effect of scattering in the drag layer. A transient measurement should be conducted to resolve the classical $\langle \mathbf{E} \rangle \times \mathbf{B}$-drift induced voltage from the momentum-transfer induced $\Delta V_{\rm drag}$ since the response time of the classical drift is far shorter than that of $\Delta V_{\rm drag}$. An overshoot of the measured voltage would signal the *negative* Coulomb drag.

Finally, we notice that the induced drag, for ν integer or half-integer, is approximately *two to three orders of magnitude larger* than that at zero field B. This is due to the fact the $B=0$ states condense into LL's when $B\neq 0$ and agrees with the results of Ref. 4.

IV. CONCLUDING REMARKS

We have shown, within a self-consistent Hartree approximation, that the current density in Coulomb-coupled *narrow* Hall bars has different current zones that change with filling factor ν. In addition to the zero-field momentum-transfer current $I_{\rm drag}$, the Hall voltage developed in the drive layer gives rise to a classical $\langle \mathbf{E} \rangle \times \mathbf{B}$-drift current $I_{\rm es}$ when the circuit is closed. As ν increases from 0.5 towards 1, $I_{\rm drag}$ or $\Delta V_{\rm drag}$ decreases and, when $\nu \rightarrow 1$, it changes sign. This change occurs because electrons make energetically favorable *near-edge inter-LL transitions*. We expect that the values of ν where the drag changes sign depend only weakly on the initial confining potential. In the present study we took the latter square well in the form and evaluated the resulting potential self-consistently. Another choice would be an initially parabolic potential, but the results would be qualitatively the same.

It is evident that the above negative drag is neither due to a thermal gradient[8] nor due to the conventional electron-hole coupling since we are dealing with electron layers. Also, since we have neglected tunneling between the layers, it cannot be identified with the observed negative drag of Ref. 12. As we suggested in Sec. IV, it could be tested with time-dependent measurements.

Finally, it should be noted that since we considered an applied current in the drive layer in the presence of scattering, i.e., a clearly *nonequilibrium* case, the resulting drag is a *dissipative* one and not the *nondissipative equilibrium* drag of Ref. 3. It is a result of the broadening of the Landau levels introduced by scattering coupled with the nonequilibrium effect as is evident from Eq. (6), in which the occupation is determined self-consistently. The scattering is embodied in $g_n(k)$. If we were to treat this system as a nondissipative one, $g_n(k)$ would be 1 and thus $I_{\rm drag}=0$. As for the use of δk in the Fermi function, to account for the nonequilibrium distribution function, it should be said that it was made, in the spirit of Ref. 9, in order to simplify the heavily involved self-consistent calculations. A thorough treatment would have to determine the distribution function from the Boltzmann equation.

ACKNOWLEDGMENTS

We would like to thank Dr. C. Dharma-wardana and Dr. H. Rubel for fruitful discussions. This work was supported by NSERC Grant Nos. OGP0003155 (H.C.W.T., D.J.W.G.) and OGP0121756 (P.V.).

[1] H. C. Tso, P. Vasilopoulos, and F. M. Peeters, Phys. Rev. Lett. **68**, 2516 (1992); **70**, 2146 (1993); Surf. Sci. **305**, 400 (1994); P. Vasilopoulos and H. C. Tso, *Condensed Matter Theories* (Plenum Press, New York, 1993), p. 81.

[2] M. B. Pogrebinskii, Fiz. Tekh. Poluprovodn. **11**, 637 (1977) [Sov. Phys. Semicond. **11**, 372 (1977)]; P. J. Price, Physica B **117**, 750 (1983); Yu. M. Sirenko and P. Vasilopoulos, Phys. Rev. B **46**, 1611 (1992); L. Zheng and A. H. MacDonald, *ibid.* **48**, 8203 (1993); K. Flensberg and B. Y. Hu, Phys. Rev. Lett. **73**, 3572 (1994).

[3] A. G. Rojo and G. D. Mahan, Phys. Rev. Lett. **68**, 2074 (1992); G. Vignale and A. H. MacDonald, *ibid.* **76**, 2786 (1996).

[4] M. C. Bonsager, K. Flensberg, B. Y. Hu, and A. Jauho, Phys. Rev. Lett. **77**, 1366 (1996); H. Rubel, A. Fischer, W. Dietsche, K. von Klitzing, and K. Eberl, *ibid.* **78**, 1763 (1997).

[5] P. M. Solomon, P. J. Price, D. J. Frank, and D. C. La Tulipe, Phys. Rev. Lett. **63**, 2508 (1989); T. J. Gramila, J. P. Eisenstein, A. H. MacDonald, L. N. Pfeiffer, and K. W. West, *ibid.* **66**, 1216 (1991); U. Sivan, P. M. Solomon, and H. Shtrikman, *ibid.* **68**, 1196 (1992).

[6] H. C. Tso and P. Vasilopoulos, Phys. Rev. B **45**, 1333 (1992); E. Shimshoni and S. L. Sondhi, *ibid.* **49**, 11 484 (1994).

[7] B. I. Halperin, Phys. Rev. B **25**, 2185 (1982).

[8] B. Laikhtman and P. M. Solomon, Phys. Rev. B **41**, 9921 (1990).

[9] C. Wexler and D. J. Thouless, Phys. Rev. B **49**, 4815 (1994).

[10] H. C. W. Tso *et al.* (unpublished).

[11] F. F. Chen, *Introduction to Plasma Physics* (Plenum Press, New York, 1977).

[12] N. K. Patel, E. H. Linfield, K. M. Brown, M. Pepper, D. A. Ritchie, and G. A. C. Jones, Semicond. Sci. Technol. **12**, 309 (1997).